図３　飲酒量別の血清中性脂肪値および脂肪肝の発生頻度

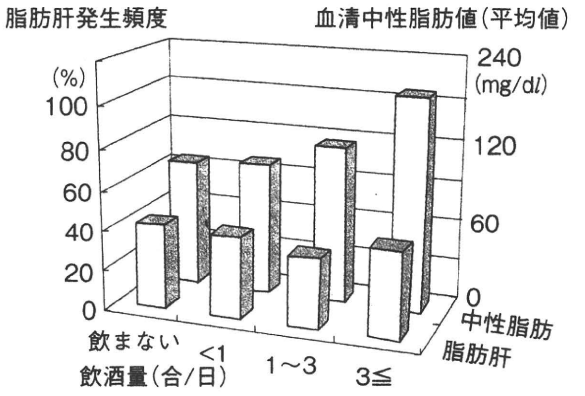


鹿児島県厚生連健康管理センターの2008年度人間ドック男性受診者（30～69歳）5,864名を対象とした．飲酒量はアンケート調査（飲酒頻度と飲む日の平均的飲酒量）に基づいて算出した．脂肪肝の診断は腹部超音波検査による．

図４　内臓肥満の発生頻度に及ぼす飲酒パターンの影響

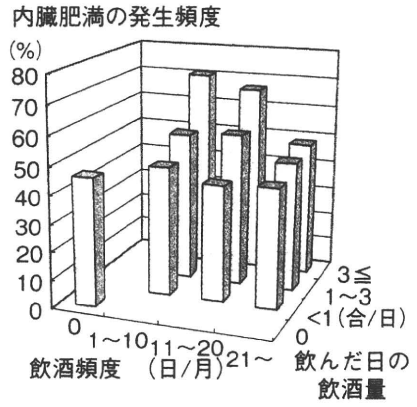


鹿児島県厚生連健康管理センターの2008年度人間ドック男性受診者（30～69歳）5,864名を対象とした．内臓肥満の診断は腹囲85 cm以上とした．

## 飲酒習慣と脂肪肝

**図3**は鹿児島県における人間ドック男性受診者について飲酒量と血清中性脂肪値や脂肪肝発生頻度の関係をみたものである．中性脂肪が飲酒量に比例して増加するにもかかわらず（127±85, 131±97, 155±162, 207±199 mg/dl, P<0.001），脂肪肝は直線的には増加しない（42.3, 40.4, 34.5, 42.9%, P<0.001）．飲酒は，中性脂肪への影響をみる限り，たしかに肝臓の脂肪合成を高めているようにみえるが，脂肪肝については，発生が抑えられているようにみえる．

Gunjiら[6]は健診受診者を対象に多変量解析（ロジスティック解析）を行い，飲酒習慣の脂肪肝発生に及ぼす影響を検討している．軽度飲酒者（20g/日未満），中等度飲酒者（20～40 g/日），高度飲酒者（40 g/日以上）について非飲酒者と比較し，脂肪肝発生のオッズ比は軽度飲酒者で0.824（P=0.044），中等度飲酒者では0.754（P=0.008）であり，飲酒習慣が脂肪肝の発生を軽減していることを報告している．また，高度飲酒者でも統計学的には有意ではないもののオッズ比は0.853（P=0.197）と1を下回る数値を示している．高度飲酒者には飲酒による脂肪肝・肝障害患者が含まれることを考えると，一方では脂肪肝のリスクを軽減している可能性が示唆される．飲酒は脂肪肝発生にとっては両刃の剣である．われわれも鹿児島県における健診受診者を対象に検討を行ったが，同様の結果であった．そのメカニズムは不明だが，飲酒と脂肪肝の関係は，飲酒量が増えると脂肪肝発生率も増えるというような単純な図式があてはまらないことは認識しておくべきである．

飲酒習慣と脂肪肝発生頻度の間の相反する関係については，飲酒がNAFLDの発生に防御的に作用している可能性もある[6~8]が，その作用機序は明確にはされていない．また，アルコール代謝には個体差があり，その影響も含めて解析しないと，たんに飲酒量だけでは飲酒の脂肪肝発生に及ぼす真の影響を明らかにできない可能性がある．

## 飲酒パターンと内臓脂肪

2008年度の男性の人間ドック受診者において飲酒パターンと腹囲85 cm以上の内臓肥満発生頻度との関係を検討したところ，1日の飲酒量が1合以上/日になると，内臓肥満の頻度が増加することが明らかになった（飲まない，47.8%；<1合/日，46.5%；1～3合，52.6；3合以上，62.5%，P<0.01，**図4**）．多変量解析では，1日の飲酒量の増加は，年齢，メタボリック症候群関

連疾患の有無などと独立した内臓肥満の危険因子であった．1日の飲酒量の増加はその日の食生活を乱し，摂取カロリーの増加をもたらし，内臓肥満を増加させる可能性を筆者は考えている．飲酒量に関連したこの内臓肥満の増加は，脂肪肝の増加につながっている．

## 飲酒に関する栄養指導

最近の脂肪肝においては，肥満や糖尿病などのメタボリック症候群関連疾患の存在がきわめて重要な役割を占めていることは間違いのない事実である．したがって，アルコール性であれ非アルコール性であれ，肥満やメタボリック症候群関連疾患が存在する場合には，これらを引き起こす生活習慣の改善をめざした栄養指導は最優先されるべき脂肪肝対策である．

アルコール代謝にともなうレドックス・シフトの解消にはオキザロ酢酸やアスパラギン酸などの十分なアミノ酸の供給が必要である．リポ蛋白（VLDL）の分泌にも十分なアミノ酸・たんぱく質が必要である．また，過度のアルコールが糖新生を阻害する．このため，アルコール性肝障害にならないためには，これらを十分にとりながら飲むことが推奨されてきた．しかし，われわれの成績では，飲酒量が1合/日を超えてくると，内臓肥満が生じ，脂肪肝の頻度が高くなる．1日に1合以上の飲酒がある場合には，むしろ食べ過ぎないような栄養指導を行うことも必要と考えられる．

先に述べたように，アルコール代謝には個体差が大きく，また肥満や生活習慣病関連疾患の合併の有無なども飲酒者によって異なることから，従来のような画一的な栄養指導では脂肪肝を減らすことは困難である．飲酒者に対する栄養指導については，生活習慣病の時代という新たな局面に入り，今後検討する課題が多い．

**参考文献**

1) Ludwig J, et al. Nonalcoholic steatohepatitis : Mayo Clinic experiences with a hitherto unnamed disease. Mayo Clin Proc 1980 ; 55(7) : 434-438.
2) You M, et al. Ethanol induces fatty acid synthesis pathways by activation of sterol regulatory element-binding protein (SREBP). J Biol Chem 2002 ; 277(32) : 29342-29347.
3) Zhou Z, et al. A critical involvement of oxidative stress in acute alcohol-induced hepatic TNF-alpha production. Am J Pathol 2003; 163(3) : 1137-1146
4) Kojima S, et al. Increase in the prevalence of fatty liver in Japan over the past 12 years : analysis of clinical background. J Gastroenterol 2003 ; 38(10) : 954-961.
5) Imamura Y, et al. Association between changes in body composition and the increasing prevalence of fatty liver in Japanese men. Hepatol Res 2008 ; 38(11) : 1083-1086.
6) Gunji T, et al. Light and moderate alcohol consumption significantly reduces the prevalence of fatty liver in the Japanese male population. Am J Gastroenterol 2009 ; 104(9) : 2189-2195.
7) Suzuki A, et al. Light to moderate alcohol consumption is associated with lower frequency of hypertransaminasemia. Am J Gastroenterol 2007 ; 102(9) : 1912-1919.
8) Dunn W, et al. Modest wine drinking and decreased prevalence of suspected non-alcoholic fatty liver disease. Hepatology 2008 ; 47(6) : 1947-1954.

*　　*　　*

疫学

# 本邦におけるNASH/NAFLDの頻度，生活習慣病を伴わないNAFLDの頻度

濵邊絢香* 宇都浩文*
今村也寸志** 坪内博仁*

索引用語：NAFLD，生活習慣病，メタボリックシンドローム，合併頻度，人間ドック

## 1 はじめに

非アルコール性脂肪性肝障害(non alcoholic fatty liver disease; NAFLD)は明らかな飲酒歴がなく，肝臓の脂肪化を特徴とする肝障害であり，以前は可逆性で予後良好な慢性疾患と考えられ，あまり重要視されていなかった．しかし，NAFLD症例の中には肝硬変や肝癌に進展する非アルコール性脂肪肝炎(non alcoholic steatohepatitis; NASH)の病態があり，NAFLDは必ずしも予後良好とはいえないことが明らかとなってきている．

「生活習慣病」(Life-style related diseases)とは，「食習慣，運動習慣，休養，喫煙，飲酒等の生活習慣が，その発症もしくは進行に関連する疾患群」であり，メタボリックシンドロームは肥満を基本病態として生活習慣病である糖尿病，高血圧，脂質異常を複数併せ持つ状態である．また，NAFLD/NASHは生活習慣病の肝病変といわれ，糖尿病などの生活習慣病の存在が，NAFLDやNASHの病態進展に促進的に作用する．食生活の欧米化やライフスタイルの変化に伴い，日本でも肥満者や生活習慣病患者が増加し，肥満や生活習慣病に伴うNAFLDの増加が危惧されている．

本稿では本邦におけるNAFLD/NASHの頻度，生活習慣病を伴わないNAFLDの頻度について概説する．

## 2 NAFLD/NASHの頻度

NAFLDの発症は人種差がみられ，黒人や白人と比べてアジア人ではNAFLDの頻度が高く，わが国のNAFLDの有病率は9～30％といわれている[1]．われわれの検討では，2008年に人間ドックを受診し，HBs抗原とHCV抗体を測定した9,013人の中で，腹部超音波検査で脂肪肝と診断された者は2,633名(29.2％)であった(図1)．また，脂肪肝症例のうちHBs抗原とHCV抗体がいずれも陰性であった受診者は2,561名(脂肪肝

*Ayaka HAMABE et al*: Epidemiology of nonalcoholic fatty liver disease with or without life-style related disease
*鹿児島大学大学院医歯学総合研究科消化器疾患生活習慣病学［〒890-8544 鹿児島県鹿児島市桜ヶ丘8-35-1］
**鹿児島厚生連病院内科

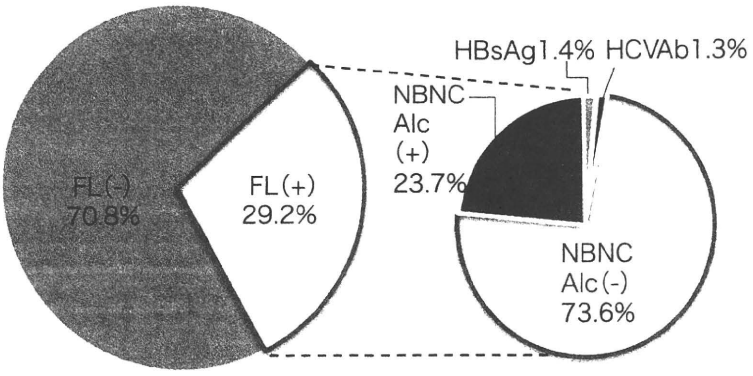


図1　人間ドック受診者における脂肪肝の頻度

FL；脂肪肝，NBNC；HBs抗原陰性かつHCV抗体陰性，Alc；アルコール，Alc(-)；1日飲酒量(エタノール換算) 20g/日以下，Alc(+)；1日飲酒量(エタノール換算) 20g/日を超える

症例の97.3％)で，さらに，アルコール摂取量がエタノール換算で20 g/日以下であったNAFLD例は1,937例(ウイルスマーカー陰性の脂肪肝症例の75.6％)である(図1)．すなわち，人間ドッグ受診者の21.5％がNAFLDと考えられる．

Kojimaらは，検診における脂肪肝の発見頻度は年々増加し，1989年では12.6％，1998年では30.3％と報告している[2]．われわれの検討で，脂肪肝におけるNAFLDの頻度は約75％であったことから，Kojimaらの報告におけるNAFLDの頻度は約23％と推測できる．また，Hamaguchiらの報告では，調査終了時のNAFLDの頻度は23.3％である[5]．このようなことから，わが国におけるNAFLDの頻度は20～25％と推定される．

NASHの頻度は成人の約1.2～4.8％と報告されている．また，Michitakaらの研究グループが行った58病院の肝硬変患者33,379人を対象とした検討では，2.1％がNASHに起因した肝硬変で，男性では1.4％，女性では3.4％と，女性に多い($p<0.0001$)[11]．一方，NASH肝硬変起因の肝癌発生率は31.5％で，男性では42.2％，女性では24.1％と男性の方が肝癌合併率は有意に高い($p<0.005$)．

## 3 性別に見たNAFLD/NASHの頻度

NAFLDの発生率には性差があり，女性より男性の方が脂肪肝になりやすく，脂肪肝の年齢分布にも性差がある．男性では30～60歳代の脂肪肝の頻度は約25％であるのに対し，女性では年齢が上がるにつれて脂肪肝の頻度は徐々に増加し，60歳代以降では男性とほぼ同率になると報告されている[2]．これには，性ホルモンが関与しており，閉経後の女性はエストロゲンの低下により内臓脂肪が蓄積し，インスリン抵抗性が引き起こされるためと考えられている[3]．そのため閉経後の女性は閉経前の女性に比べNAFLDのリスクが高いと報告されている．また，われわれの検討では，男性は脂肪肝の頻度が増加傾向であるのに対して，女性の脂肪肝の頻度は2000年と2005年では差がない(図2)．男性は今後も脂肪肝の増加が危惧されるが，女性で今後増加するかはさらなる解析が必要である．

## 4 肥満とNAFLD，NASH

平成19年度国民健康・栄養調査によると，肥満度[BMI(kg/m$^2$)＝体重(kg)/身長$^2$(m$^2$)]25 kg/m$^2$以上の肥満者の割合は，20年前，

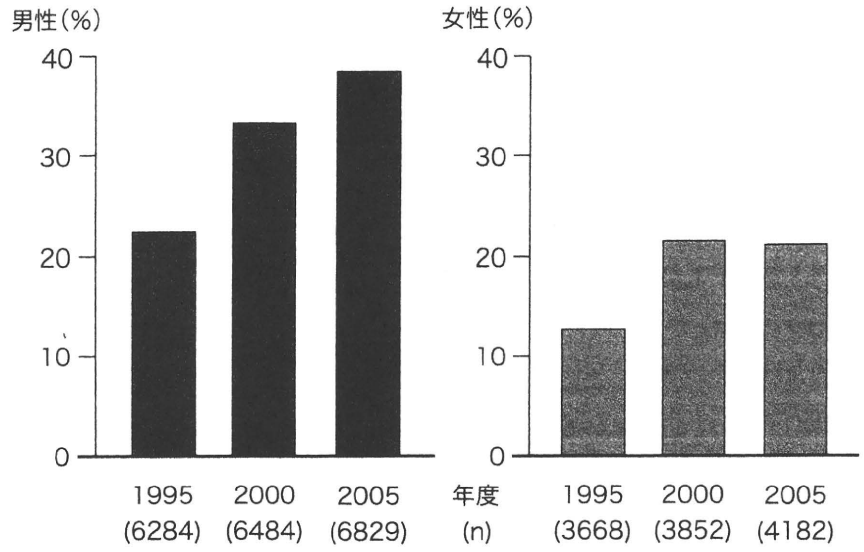


図2　1995年，2000年および2005年人間ドック受診者における脂肪肝の頻度
（飲酒者を含む）

10年前と比べて男性は増加傾向にある．また，男性も女性も肥満の頻度は年代とともに徐々に上昇している．

肥満は脂肪肝の最も重要な危険因子と考えられている．BMIが23未満の非肥満者の脂肪肝の頻度はわずか2.7％であるが，23≦BMI＜25では10.5％，25≦BMI＜30の肥満者では34.6％，30≦BMIの高度肥満者では77.6％と，肥満の程度の増加に伴い脂肪肝は増加する[4]．また，Kojimaらは1989～2000年の12年間東海大学病院健診センターの受診者39,151人を解析し，脂肪肝の有病率はBMIが25未満の非肥満者では12.8％，25≦BMI＜30の肥満者では51.4％，BMIが30以上の高度肥満者では80.4％と，肥満の程度は脂肪肝の発症に相関し，BMIが25以上である場合，非肥満者と比較して脂肪肝のリスクはオッズ比6.3であると報告している[2]．

HamaguchiらはNAFLDとメタボリックシンドロームの関連について前向き研究を行い，調査開始時にはNAFLDは18％にみられ，平均約13.8カ月の追跡期間で新たに10％（男性では14％，女性では5％）の発症があったと報告している．新たにNAFLDが発症した症例は男性では1.7±1.7 kg，女性では1.3±1.4 kgの体重増加がみられ，ロジスティック回帰分析において，体重の増加はNAFLDの独立した危険因子で，男性ではOR 1.51（95％ CI 1.40, 1.63），女性ではOR 1.62（95％ CI 1.39, 1.89）である[5]．

さらに，近年は小児の肥満が増加しており，小児のNAFLDも問題となっている．Tominagaらは6～15歳を対象としたNAFLDの有病率を検討し，6～10歳では3.4％，11歳から15歳では5.2％と報告した[6]．また，小児メタボリックシンドローム診断基準の該当者におけるNAFLDの頻度は，予備群該当者では40.0％，基準該当者では76.8％であり，メタボリックシンドロームはNAFLDの独立した危険因子である．Tsurutaらも中学生288人を対象に同様の検討を行い，2007年の肥満者は5.9％，NAFLDの有病率は4.5％であると報告した[7]．さらに，肥満（肥満度［（体重－標準体重）／標準体重×100］≧20％）の合併率は，NAFLDでは58.3％，非NAFLDでは5.7％と有意に頻度が異なる（p≦0.001）．

## 5 糖尿病とNAFLD，NASH

本邦において，糖尿病が強く疑われる人（HbA1c≧6.1％または，現在治療中）は890万人，糖尿病の可能性が否定できない人（5.6％≦HbA1c＜6.1％）が1,320万人で合計2,210万人が糖尿病の可能性があり，10年前と比較して1.6倍増加している[8]．Kojimaらの検討では，正常型（FBS＜110 mg/dl）の脂肪肝の有病率は18.6％，境界型（110≦FBS＜126 mg/dl）は43.7％，糖尿病型（FBS≧126 mg/dl）は53.3％と有意な差がみられ，FBS≧110 mg/dlは脂肪肝の独立した危険因子である（OR；3.1）[2]．同様にJimbaらも埼玉県の健康診断受診者1,950人を解析している．全体のNAFLDの有病率は29％であり，NAFLDと糖代謝の関係では，NAFLDの有病率は正常型（FPG＜6.1 mmol/l）は27％，境界型（6.1 mmol/l≦FPG＜7.0 mmol/l）は43％，糖尿病型（FPG≧7.0 mmol/lまたは糖尿病歴あり）は62％である．また，糖代謝異常（境界型および糖尿病型）の合併率はNAFLDでは19.1％，非NAFLDでは5.6％と有意差を認めている（p＜0.001）[9]．

Hisamatsuらは182人のNAFLD患者を対象に，肝線維化の危険因子について検討している．糖尿病の合併は軽度線維化群では42％，重度線維化（架橋線維化以上）群では71％と有意差があり（p＝0.005），多変量解析における糖尿病のORは2.97（95％ CI：1.24，7.12）であり，糖尿病は肝の線維化にも関与していると考えられる[10]．

## 6 生活習慣病を伴わないNAFLDの頻度

生活習慣病である肥満，糖尿病，高血圧，脂質異常症を伴わない場合のNAFLDの発生率は約25％といわれ，リスクファクターが1つあると43％，2つでは72％と，生活習慣病の合併に伴い脂肪肝の頻度は高くなる．また，NAFLDの頻度は肥満があると50～80％，糖尿病では40～50％，脂質異常症では42～58％と報告されている[1]．さらに，NASHに起因した肝硬変では平均BMIは27.6±4.5と肥満が多く，高血圧，糖尿病の合併率はそれぞれ50.2％，66.6％であった[11]．

Hamaguchiらの検討では，メタボリックシンドロームの存在は新たなNAFLDの発症にも関与し，男性OR 4.00（95％ CI 2.63, 6.08），女性OR 11.20（95％ CI 4.85, 25.87）と高いNAFLDの発症危険因子であり，メタボリックシンドロームとNAFLDは密接に関連すると考えられる[5]．

われわれのデータでは，NAFLDのうち，肥満の合併は55.2％，高血圧は50.9％，糖尿病は36.9％，脂質異常症は69.0％であり，non-NAFLDではそれぞれ12.9％，36.3％，18.2％，36.6％で，NAFLDは生活習慣病を合併する頻度がnon-NAFLDより高い（図3）．また，肥満，高血圧，糖尿病，脂質代謝異常を全く伴わない場合のNAFLDの発生率は6.7％と極めて少なく，生活習慣病の合併数が増加するに従って，NAFLDの頻度は増加し，1つ該当すると21.2％，2つ該当すると38.3％，3つ以上該当すると63.1％である（図4）．また，前述のとおり，肥満などの生活習慣病を全く伴わない検診受診者の中ではNAFLDの頻度は6.7％，検診受診者全体のなかでのNAFLDの頻度は1.4％であり，生活習慣病を伴わないNAFLDの頻度は非常に少ないと考えられる．

## 7 おわりに

肥満や糖尿病などメタボリックシンドロームを背景病変としたNAFLDやNASHは，今

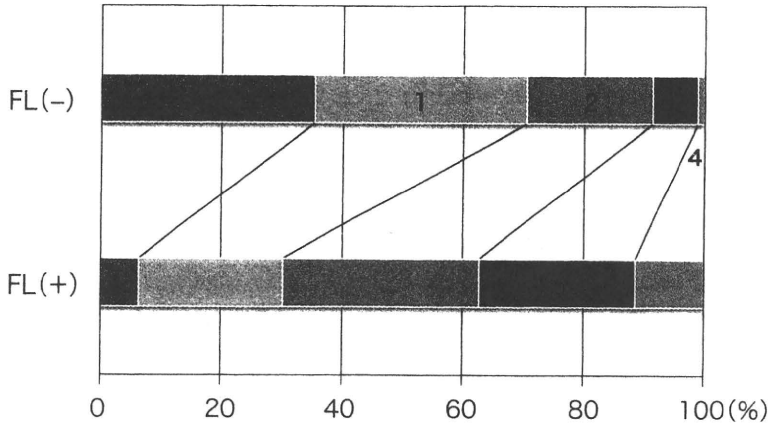


図3　生活習慣病(肥満，高血圧，糖尿病，脂質異常症)の合併数とNAFLDの頻度
FL(+)；NAFLDあり，FL(−)；NAFLDなし

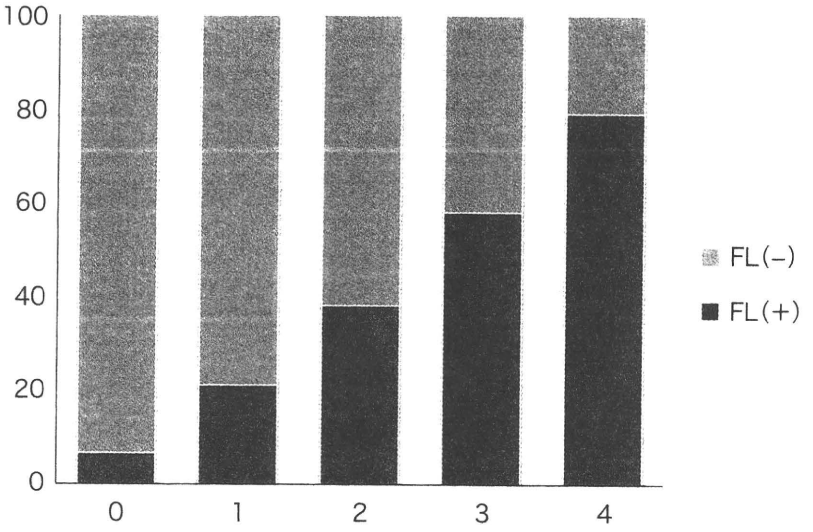


図4　生活習慣病(肥満，高血圧，糖尿病，脂質異常症)合併数別に見たNAFLDの頻度
FL(−)；NAFLDなし，FL(+)；NAFLDあり

後もメタボリックシンドローム人口の増加とともに，ますます増加すると考えられる．一方，生活習慣病を伴わないNAFLDは稀と考えられるが，その病態が生活習慣病を伴うNAFLDと同じかは十分明らかになっていない．生活習慣病を伴うNAFLDにおける治療はまず肥満の治療を基本とした生活習慣病の改善であるが，生活習慣病を伴わないNAFLDにおける治療法についてはさらに検討が必要である．

## 文　献

1) Deepak NA, Hashimoto E, Laurentius AL et al : How common is non-alcoholic fatty liver disease in the Asia-Pacific region and are there local differences? J Gastroenterol Hepatol 22 : 788–793, 2007
2) Kojima S, Watanabe N, Numata M et al : Increase in the prevalence of fatty liver in Japan over the past 12 years: analysis of clinical background. J Gastroenterol 38 : 954–961, 2003
3) Suzuki A, Manal FA : Nonalcholic fatty liver disease in women. Women's Health 5 (2) : 191–203, 2009
4) 西原利治：NASH診療best approach．中外医学

社，東京，2008
5) Hamaguchi M, Kojima T, Takebe N et al : The metabolic syndrome as a predictor of nonalcoholic fatty liver disease. Ann Int Med 143 : 722–728, 2005
6) Tominaga K, Fujimoto E, Suzuki K et al : Prevalence of non-alcoholic fatty liver disease in children and relationship to metabolic syndrome, insulin resistance, and waist circumference. Environ Health Prev Med 14 : 142–149, 2009
7) Tsuruta G, Tanaka N, Hongo M et al : Nonalcoholic fatty liver disease in Japanese junior high school students: its prevalence and relationship to lifestyle habits. J Gastroenterol 2010（in press）
8) 厚生労働省 健康局総務課生活習慣病対策室：平成19年国民健康・栄養調査報告
9) Jimba S, Nakagami T, Takahashi M et al : Prevalence of non-alcoholic fatty liver disease and its association with impaired glucose metabolism in Japanese adults. Diabetic Med 22 : 1141–1145, 2005
10) Hisamatsu M, Ichikawa T, Nakao K et al : Clinicopathological study of nonalcoholic fatty liver disease in Japan: the risk factors for fibrosis. Liver International 28 : 519–524, 2008
11) Michitaka K, Nishiguchi S, Aoyagi Y et al : Etiology of liver cirrhosis in Japan : a nationwide survey. J Gastroenterol 45 : 86–94, 2010

*　　*　　*

OPEN ACCESS Freely available online

PLoS one

# The Progression of Liver Fibrosis Is Related with Overexpression of the miR-199 and 200 Families

**Yoshiki Murakami[1]*, Hidenori Toyoda[2], Masami Tanaka[3], Masahiko Kuroda[3], Yoshinori Harada[4], Fumihiko Matsuda[1], Atsushi Tajima[5¤], Nobuyoshi Kosaka[6], Takahiro Ochiya[6], Kunitada Shimotohno[7]**

**1** Center for Genomic Medicine, Kyoto University Graduate School of Medicine, Kyoto, Japan, **2** Department of Gastroenterology, Ogaki Municipal Hospital, Ogaki, Japan, **3** Department of Molecular Pathology, Tokyo Medical University, Tokyo, Japan, **4** Department of Pathology and Cell Regulation, Kyoto Prefectural University of Medicine, Kyoto, Japan, **5** Department of Molecular Life Science, Tokai University School of Medicine, Isehara, Japan, **6** Division of Molecular and Cellular Medicine, National Cancer Center Research Institute, Tokyo, Japan, **7** Research Institute, Chiba Institute of Technology, Narashino, Japan

## Abstract

***Background:*** Chronic hepatitis C (CH) can develop into liver cirrhosis (LC) and hepatocellular carcinoma (HCC). Liver fibrosis and HCC development are strongly correlated, but there is no effective treatment against fibrosis because the critical mechanism of progression of liver fibrosis is not fully understood. microRNAs (miRNAs) are now essential to the molecular mechanisms of several biological processes. In order to clarify how the aberrant expression of miRNAs participates in development of the liver fibrosis, we analyzed the liver fibrosis in mouse liver fibrosis model and human clinical samples.

***Methodology:*** In a $CCL_4$-induced mouse liver fibrosis model, we compared the miRNA expression profile from $CCL_4$ and olive oil administrated liver specimens on 4, 6, and 8 weeks. We also measured expression profiles of human miRNAs in the liver biopsy specimens from 105 CH type C patients without a history of anti-viral therapy.

***Principle Findings:*** Eleven mouse miRNAs were significantly elevated in progressed liver fibrosis relative to control. By using a large amount of human material in CH analysis, we determined the miRNA expression pattern according to the grade of liver fibrosis. We detected several human miRNAs whose expression levels were correlated with the degree of progression of liver fibrosis. In both the mouse and human studies, the expression levels of miR-199a, 199a*, 200a, and 200b were positively and significantly correlated to the progressed liver fibrosis. The expression level of fibrosis related genes in hepatic stellate cells (HSC), were significantly increased by overexpression of these miRNAs.

***Conclusion:*** Four miRNAs are tightly related to the grade of liver fibrosis in both human and mouse was shown. This information may uncover the critical mechanism of progression of liver fibrosis. miRNA expression profiling has potential for diagnostic and therapeutic applications.

**Citation:** Murakami Y, Toyoda H, Tanaka M, Kuroda M, Harada Y, et al. (2011) The Progression of Liver Fibrosis Is Related with Overexpression of the miR-199 and 200 Families. PLoS ONE 6(1): e16081. doi:10.1371/journal.pone.0016081

**Editor:** Chad Creighton, Baylor College of Medicine, United States of America

**Received** September 15, 2010; **Accepted** December 6, 2010; **Published** January 24, 2011



**Funding:** This work was supported by the Japanese Ministry of Health, Labour and Welfare (Y.M, and K.S). This work was also supported by the 'Strategic Research-Based Support' Project for private universities; with matching funds from the Ministry of Education, Culture, Sports, Science and Technology (M.K). The funders had no role in study design, data collection and analysis, decision to publish, or preparation of the manuscript.

**Competing Interests:** The authors have declared that no competing interests exist.

* E-mail: ymurakami@genome.med.kyoto-u.ac.jp

¤ Current address: Department of Human Genetics and Public Health, Institute of Health Biosciences, The University of Tokushima Graduate School, Tokushima, Japan

## Introduction

Chronic viral hepatitis is a major risk factor for hepatocellular carcinoma (HCC) [1]. Worldwide 120–170 million persons are currently chronically Hepatitis C Virus (HCV) infected [2]. Due to repetitive and continuous inflammation, these patients are at increased risk of developing cirrhosis, subsequent liver decompensation and/or hepatocellular carcinoma. However, the current standard of care; pegylated interferon and rivabirin combination therapy is unsatisfied in the patients with high titre of HCVRNA and genotype 1b. Activated human liver stellate cells (HSC) with chronic viral infection, can play a pivotal role in the progression of liver fibrosis [3]. Activated HSC produce a number of profibrotic cytokines and growth factors that perpetuate the fibrotic process through paracrine and autocrine effects.

MicroRNAs (miRNAs) are endogenous small non-coding RNAs that control gene expression by degrading target mRNA or suppressing their translation [4]. There are currently 940 identifiable human miRNAs (The miRBase Sequence Database - Release ver. 15.0). miRNAs can recognize hundreds of target genes with incomplete complementary; over one third of human genes appear to be conserved miRNA targets [5][6]. miRNA is associated several pathophysiologic events as well as fundamental cellular processes such as cell proliferation and differentiation. Aberrant expression of miRNA can be associated with the liver diseases [7][8][9][10]. Recently reported miRNAs can regulate the activation of HSCs and thereby regulate liver fibrosis. miR-29b, a negative regulator for the type I collagen and SP1, is a key regulator of liver fibrosis [11]. miR-27a and 27b allowed culture-activated rat HSCs to switch to a more quiescent HSC phenotype,

with restored cytoplasmic lipid droplets and decreased cell proliferation [12].

In this study, we aimed to reveal the association between miRNA expression patterns and the progression of liver fibrosis by using a chronic liver inflammation model in mouse. We also sought to identify the miRNA expression profile in chronic hepatitis (CH) C patients according to the degree of liver fibrosis, and to clarify how miRNAs contribute to the progression of liver fibrosis. We observed a characteristic miRNA expression profile common to both human liver biopsy specimens and mouse $CCL_4$ specimens, comprising the key miRNAs which are associated with the liver fibrosis. This information is expected to uncover the mechanism of liver fibrosis and to provide a clearer biomarker for diagnosis of liver fibrosis as well as to aid in the development of more effective and safer therapeutic strategies for liver fibrosis.

## Results

### The expression level of several mouse miRNAs was increased by introducing mouse liver fibrosis

In order to identify changes in the miRNA expression profile between advanced liver fibrosis and non-fibrotic liver, we intraperitoneally administered $CCL_4$ in olive oil or olive oil alone twice a week for 4 weeks and then once a week for the next 4 weeks. Mice were sacrificed at 4, 6, or 8 weeks and then the degree of mouse liver fibrosis was determined by microscopy (Figure S1). miRNA expression analysis was performed from the liver tissue collected at the same time. Histological examination revealed that the degree of liver fibrosis progressed in mice that received $CCL_4$ relative to mice receiving olive oil alone (Figure 1A). Microarray analysis revealed that in $CCL_4$ mice, the expression level of 11 miRNAs was consistently higher than that in control mice (Figure 1B).

### miRNA expression profile in each human liver fibrosis grade

We then established human miRNAs expression profile by using 105 fresh-frozen human chronic hepatitis (CH) C liver tissues without a history of anti-viral therapy, classified according to the grade of the liver fibrosis (F0, F1, F2, and F3 referred to METAVIR fibrosis stages)(Figure 2, Table S2). Fibrosis grade F0 was considered to be the negative control because these samples were derived from patients with no finding of liver fibrosis. In zebrafish, most highly tissue-specific miRNAs are expressed during embryonic development; approximately 30% of all miRNAs are expressed at a given time point in a given tissue [13]. In mammals, the 20–30% miRNA call rate has recently been validated [14]. Such analysis revealed that the diversity of miRNA expression level among specimens was small. Therefore, we focused on miRNAs with a fold change in mean expression level greater than 1.5 ($p<0.05$) in the two arbitrary groups of liver fibrosis.

Expression of several miRNAs was dramatically different among grades of fibrosis. In the mice study 11 miRNAs were related to the progression of liver fibrosis (mmu-let-7e, miR-125-5p, 199a-5p, 199b, 199b*, 200a, 200b, 31, 34a, 497, and 802). In the human study 10 miRNAs were extracted, and the change in their expression level varied significantly between F0 and F3 (F0<F3: hsa-miR-146b, 199a, 199a*, 200a, 200b, 34a, and 34b, F0>F3: hsa-miR-212, 23b, and 422b). The expression level of 6 miRNAs was significantly different between F0 and F2 (F0<F2: hsa-miR-146b, 200a, 34a, and 34b, F0>F2: hsa-miR-122 and 23b). 5 extracted miRNAs had an expression level that was significantly different between F1 and F2 (F1<F2: hsa-miR-146b, F1>F2: hsa-miR-122, 197, 574, and 768-5p). The expression level of 9 miRNAs changed significantly between F1 and F3 (F1<F3: hsa-miR-146b, 150, 199a, 199a*, 200a, and 200b, F1>F3: hsa-miR-378, 422b, and 768-5p). The miRNAs related to liver fibrosis were extracted using two criteria: similar expression pattern in both the human and the mice specimens and shared sequence between human and mouse. We compared the sequences of mouse miRNAs as described on the Agilent Mouse MiRNA array Version 1.0 (miRbase Version 10.1) and human miRNAs as described on the Agilent Human MiRNA array Version 1.5 (miRbase Version 9.1). The sequences of mmu-miR-199a-5p, mmu-miR-199b, mmu-miR-199b, mmu-miR-200a, and mmu-miR-200b in mouse miRNA corresponded to the sequences of hsa-miR-199a, hsa-miR-199a*, hsa-miR-199a, hsa-miR-200a, and hsa-miR-200b in human miRNA, respectively (Table S3).

### Validation of the microarray result by real-time qPCR

The 4 human miRNAs (miR-199a, miR-199a*, miR-200a, and miR-200b) with the largest difference in fold change between the F1 and F3 groups were chosen to validate the microarray results using stem-loop based real-time qPCR. The result of real-time qPCR supported the result of that microarray analysis. The expression level of these 4 miRNAs was significantly different between F0 and F3 and spearman correlation analysis also showed that the expressions of these miRNAs were strongly and positively correlated with fibrosis grade ($n = 105$, $r = 0.498$(miR-199a), 0.607(miR-199a*), 0.639(miR-200a), 0.618(miR-200b), p-values<0.0001) (Figure 3).

### Over expression of miR-199a, 199a*, 200a, and 200b was associated with the progression of liver fibrosis

In order to reveal the function of miR-199a, miR-199a*, miR-200a, and miR-200b, we investigated the involvement of these miRNAs in the modulation of fibrosis-related gene in LX-2 cells. The endogenous expression level of these 4 miRNAs in LX2 and normal liver was low according to the microarray study (Figure S2). Transforming growth factor (TGF)β is one of the critical factors for the activation of HSC during chronic inflammation [15] and TGFβ strongly induced expression of three fibrosis-related genes include a matrix degrading complex comprised of α1 procollagen, matrix remodeling complex, comprised of metalloproteinases-13 (MMP-13), tissue inhibitors of metalloproteinases-1 (TIMP-1) in LX-2 cells (Figure 4A). Furthermore, overexpression of miR-199a, miR-199a*, miR-200a and miR-200b in LX-2 cells resulted significant induction of above fibrosis-related genes compared with control miRNA (Figure 4B). Finally we validated the involvement of TGFβ in the modulation of these miRNAs. In LX-2 cells treated with TGFβ, the expression levels of miR-199a and miR-199a* were significantly higher than in untreated cells; the expression levels of miR-200a and miR-200b were significantly lower than in untreated cells. Thus, our in vitro analysis suggested a possible involvement of miR-199a, 199a*, 200a, and 200b in the progression of liver fibrosis.

## Discussion

Our comprehensive analysis showed that the aberrant expression of miRNAs was associated with the progression of liver fibrosis. We identified that 4 highly expressed miRNAs (miR-199a, miR-199a*, miR-200a, and miR-200b) that were significantly associated with the progression of liver fibrosis both human and mouse. Coordination of aberrant expression of these miRNAs may contribute to the progression of liver fibrosis.

Prior studies have discussed the expression pattern of miRNA found in liver fibrosis samples between previous and present study. In this report and prior mouse studies and the expression pattern of

A

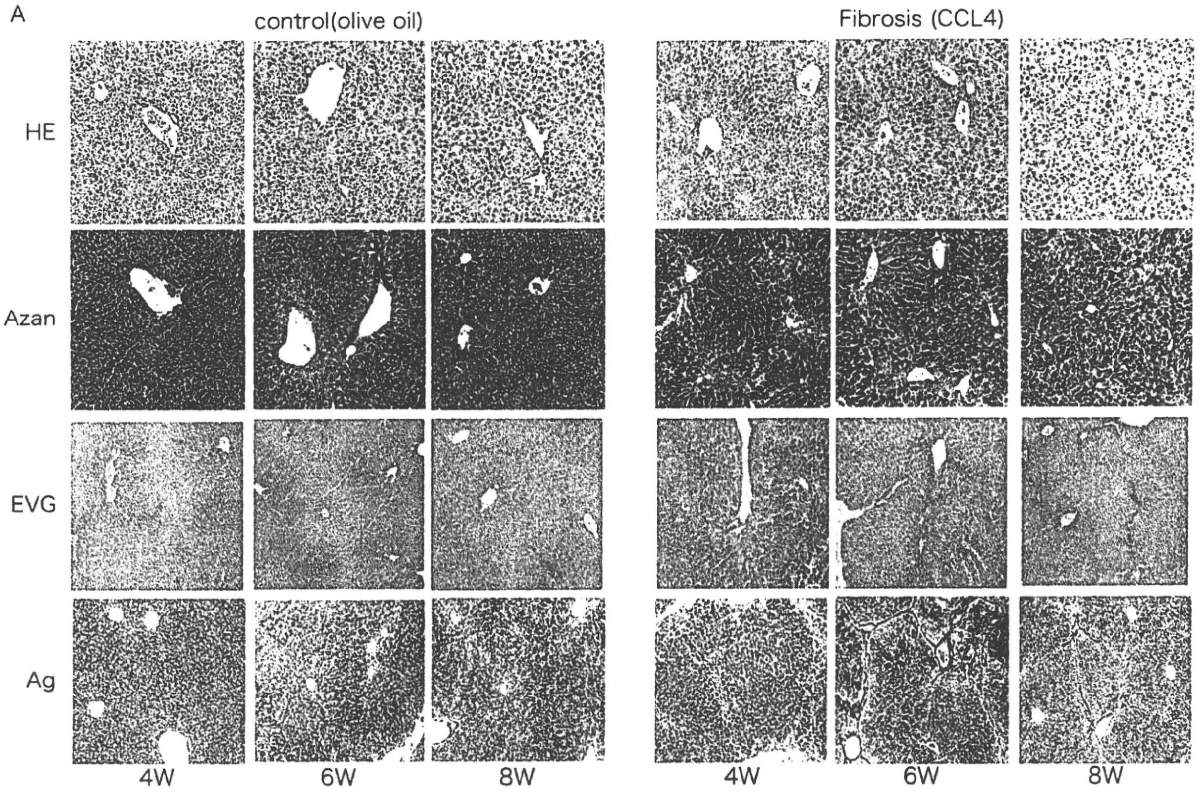


B

| miRNA | Fold change CCL4 mouse/control | | |
|---|---|---|---|
| | 4week | 6week | 8week |
| mmu-let-7e | 2.92 | 2.09 | 2.64 |
| mmu-miR-125a-5p | 4.29 | 2.35 | 2.67 |
| mmu-miR-199a-5p | 2.71 | 2.12 | 2.38 |
| mmu-miR-199b | 3.25 | 2.55 | 2.49 |
| mmu-miR-199b* | 5.13 | 4.47 | 3.94 |
| mmu-miR-200a | 2.23 | 1.63 | 2.02 |
| mmu-miR-200b | 2.38 | 2.06 | 2.20 |
| mmu-miR-31 | 3.4 | 2.35 | 3.19 |
| mmu-miR-34a | 3.89 | 3.22 | 3.5 |
| mmu-miR-497 | 2.25 | 2.00 | 2.55 |
| mmu-miR-802 | 2.02 | 2.87 | 2.74 |

**Figure 1. The change of liver fibrosis in mouse model.** A. Representative H&E-stained, Azan-stained, Ag-stained, and EVG-stained histological sections of liver from mice receiving olive oil alone or $CCL_4$ in olive oil. Magnification is ×10. B. The expression level of mmu-miRNA in mouse liver with olive oil or $CCL_4$ at 4W, 6W, and 8W respectively, by microarray analysis.
doi:10.1371/journal.pone.0016081.g001

3 miRNAs (miR-199a-5p, 199b*, 125-5p) was found to be similar while the expression pattern of 11 miRNAs (miR-223, 221, 24, 877, 29b, 29a, 29c, 30c, 365, 148a, and 193) was partially consistent with fibrosis grade [16]. In low graded liver fibrosis, the low expression pattern of 3 miRNAs (miR-140, 27a, and 27b) and the high expression pattern of 6 miRNAs in rat miRNAs (miR-29c*, 143, 872, 193, 122, and 146) in rat miRNA was also similar to our mouse study (GEO Series accession number GSE19865) [11] [12] [17].

The results in this study and previously completed human studies reveal that the expression level of miR-195, 222, 200c, 21, and let-7d was higher in high graded fibrotic liver tissue than in low graded fibrotic liver tissue. Additionally, the expression level of miR-301, 194, and 122 was lower in the high graded fibrotic liver tissue than in low graded fibrotic liver tissue [18] [19] [20](GEO Series accession number GSE16922). This difference in miRNA expression pattern may be contributed to (1) the difference of microarray platform, (2) difference of analytic procedure, and (3) the difference of the species (rat, mouse, and human).

The miR-199 and miR-200 families have are circumstantially related to liver fibrosis. TGFβ-induced factor (TGIF) and SMAD

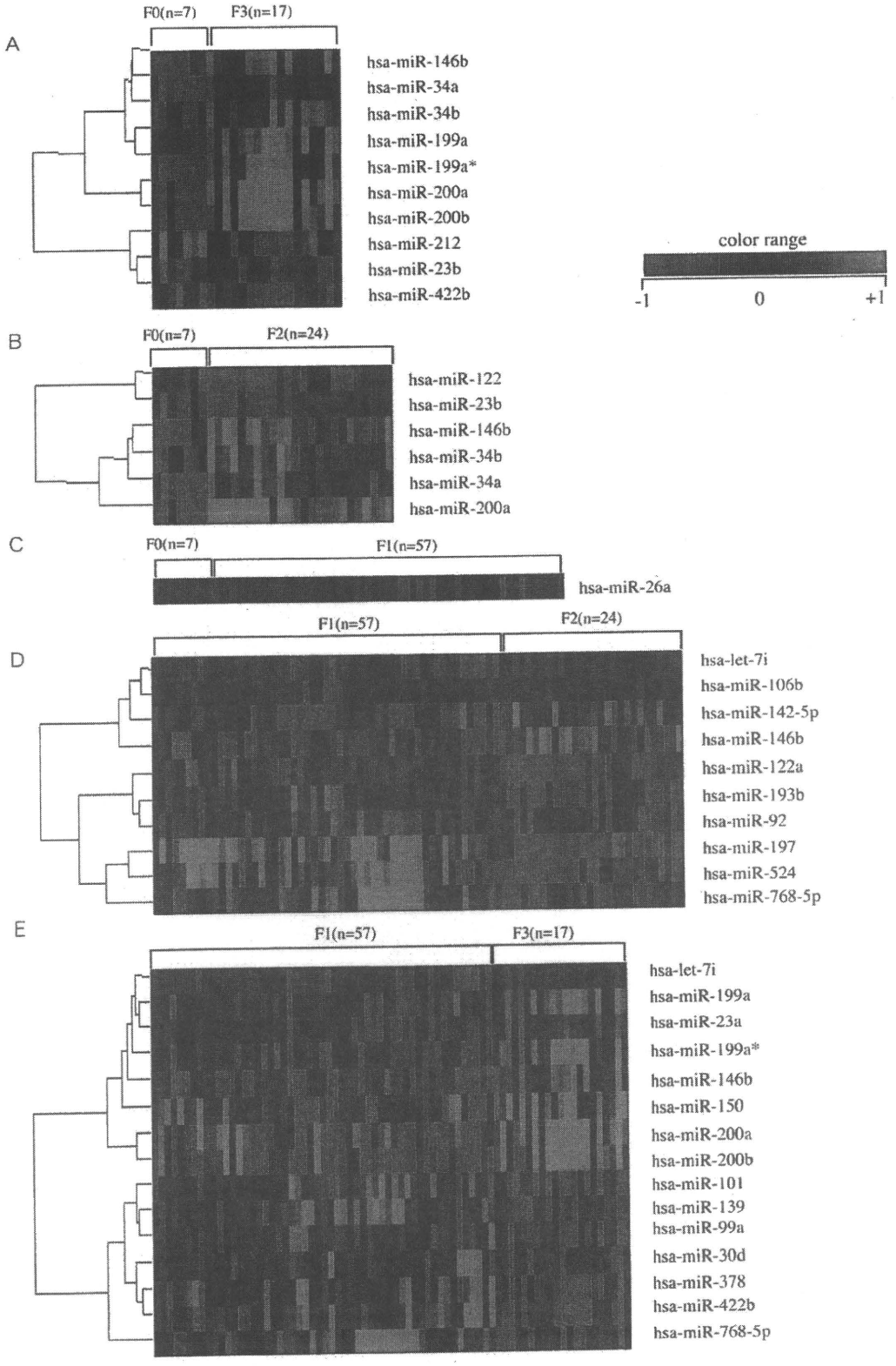
A
F0(n=7)
F3(n=17)
hsa-miR-146b
hsa-miR-34a
hsa-miR-34b
hsa-miR-199a
hsa-miR-199a*
hsa-miR-200a
hsa-miR-200b
hsa-miR-212
hsa-miR-23b
hsa-miR-422b
color range
-1
0
+1
B
F0(n=7)
F2(n=24)
hsa-miR-122
hsa-miR-23b
hsa-miR-146b
hsa-miR-34b
hsa-miR-34a
hsa-miR-200a
C
F0(n=7)
F1(n=57)
hsa-miR-26a
D
F1(n=57)
F2(n=24)
hsa-let-7i
hsa-miR-106b
hsa-miR-142-5p
hsa-miR-146b
hsa-miR-122a
hsa-miR-193b
hsa-miR-92
hsa-miR-197
hsa-miR-524
hsa-miR-768-5p
E
F1(n=57)
F3(n=17)
hsa-let-7i
hsa-miR-199a
hsa-miR-23a
hsa-miR-199a*
hsa-miR-146b
hsa-miR-150
hsa-miR-200a
hsa-miR-200b
hsa-miR-101
hsa-miR-139
hsa-miR-99a
hsa-miR-30d
hsa-miR-378
hsa-miR-422b
hsa-miR-768-5p

**Figure 2. Liver fibrosis in human liver biopsy specimen.** A. B. C. D. and E. miRNAs whose expression differs significantly between F0 and F3, F0 and F1, F0 and F2, F1 and F2, and F1 and F3, respectively. Relative expression level of each miRNA in human liver biopsy specimen by microarray. Data from microarray were also statistically analyzed using Welch's test and the Bonferroni correction for multiple hypotheses testing. Fold change, p-value are listed in Table S2.
doi:10.1371/journal.pone.0016081.g002

specific E3 ubiquitin protein ligase 2 (SMURF2), both of which play roles in the TGFβ signaling pathway, are candidate targets of miR-199a* and miR-200b, respectively, as determined by the Targetscan algorithm. The expression of miR-199a* was silenced in several proliferating cell lines excluding fibroblasts [21]. Down regulation of miR-199a, miR-199a* and 200a in chronic liver injury tissue was associated with the hepatocarcinogenesis [9]. miR-199a* is also one of the negative regulators of the HCV replication [22]. According to three target search algorithms (Pictar, miRanda, and Targetscan), the miRNAs that may be associated with the liver fibrosis can regulate several fibrosis-related genes (Table S4). Aberrant expression of these miRNAs may be closely related to the progress of the chronic liver disease.

Epithelial-mesenchymal transition (EMT) describes a reversible series of events during which an epithelial cell loses cell-cell contacts and acquires mesenchymal characteristics [23]. Although EMT is not a common event in adults, this process has been implicated in such instances as wound healing and fibrosis. Recent reports showed that the miR-200 family regulated EMT by targeting EMT accelerator ZEB1 and SIP1 [24]. From our observations, overexpression of miR-200a and miR-200b can be connected to the progression of liver fibrosis.

The diagnosis and quantification of fibrosis have traditionally relied on liver biopsy, and this is still true at present. However, there are a number of drawbacks to biopsy, including the invasive nature of the procedure and inter-observer variability. A number of staging systems have been developed to reduce both the inter-observer variability and intra-observer variability, including the METAVIR, the Knodell fibrosis score, and the Scheuer score. However, the reproducibility of hepatic fibrosis and inflammatory activity is not as consistent [25]. In fact, in our study, the degree of fibrosis of the two arbitrary fibrosis groups was classified using the miRNA expression profile with 80% or greater accuracy (data not shown). Thus, miRNA expression can be used for diagnosis of liver fibrosis.

In this study we investigated whether common miRNAs in human and mouse could influence the progression of the liver fibrosis. The signature of miRNAs expression can also serves as a tool for understanding and investigating the mechanism of the onset and progression of liver fibrosis. The miRNA expression profile has the potential to be a novel biomarker of liver fibrosis.

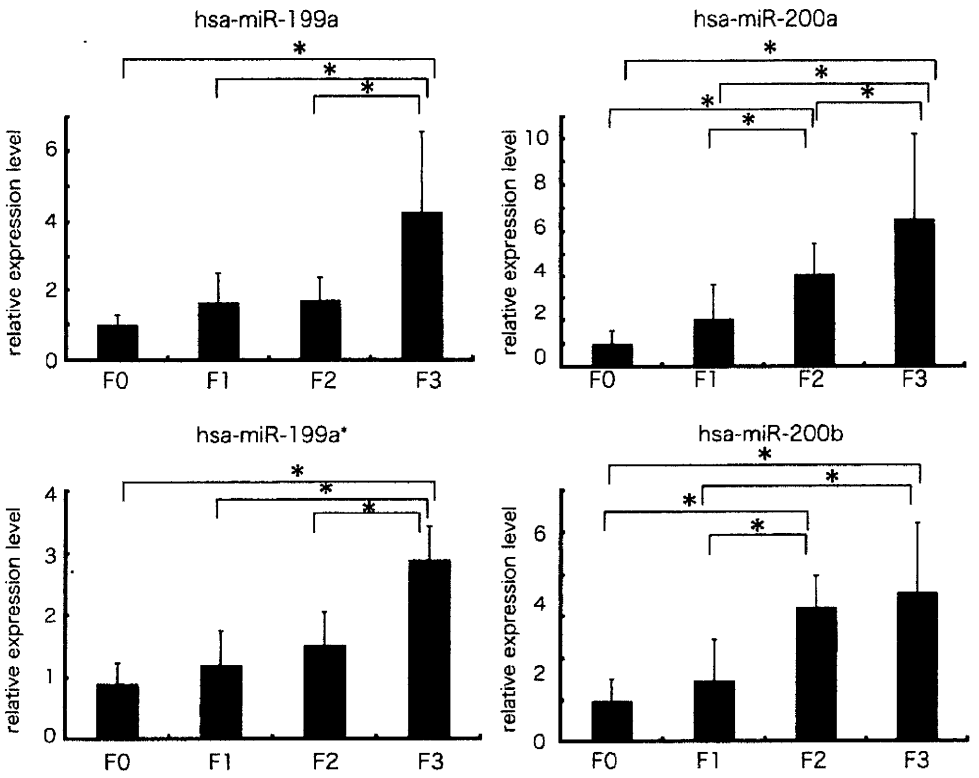


**Figure 3. The expression level of miR-199 and 200 families in human liver biopsy specimen by real-time qPCR.** Real-time qPCR validation of the 4 miRNAs (miR-199a, miR-199a*, miR-200a, and miR-200b). Each column represents the relative amount of miRNAs normalized to the expression level of U18. The data shown are the means+SD of three independent experiments. Asterisks indicates to a significant difference of $p<0.05$ (two-tailed Student-t test), respectively.
doi:10.1371/journal.pone.0016081.g003

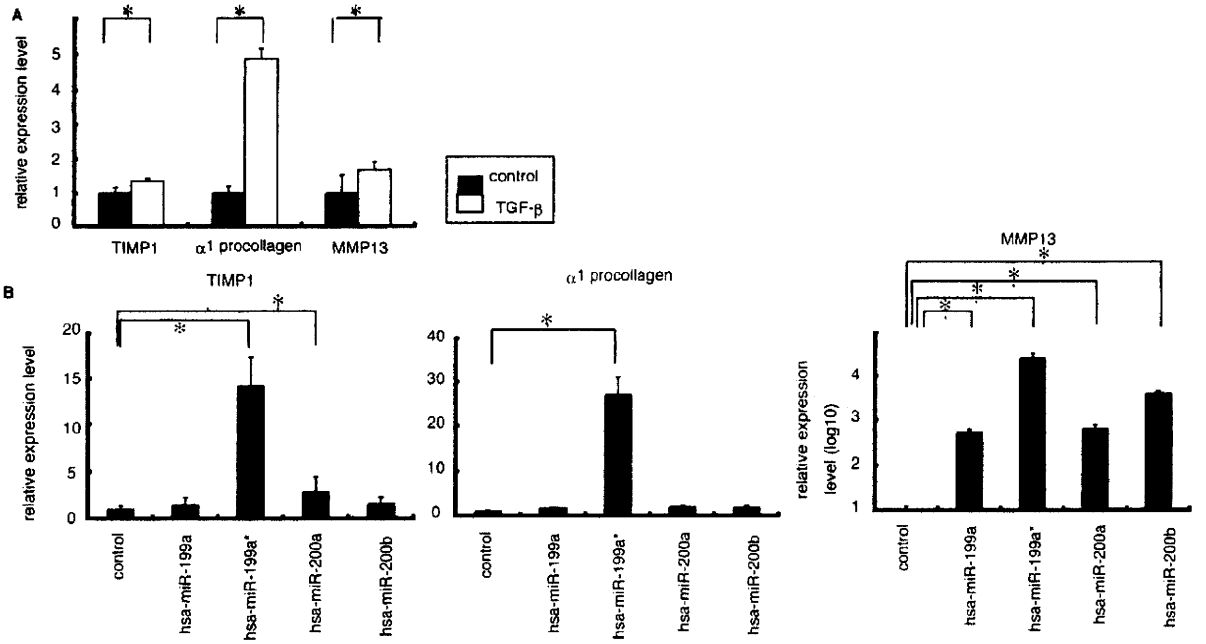


**Figure 4. The relationship between expression level of miR-199 and 200 families and expression level of three fibrosis related genes.** A. Administration of TGFβ in LX2 cells showed that the expression level of three fibrosis related genes were higher than that in non-treated cells. The data shown are the means+SD of three independent experiments. Asterisk was indicated to the significant difference of $p<0.05$ (two-tailed Student-t test). B. The expression levels of 3 fibrosis related genes in LX2 cells with overexpressing miR-199a, 199a*, 200a, or 200b, respectively were significantly higher than that in cells transfected with control miRNA ($p<0.05$; two-tailed Student t-test).
doi:10.1371/journal.pone.0016081.g004

Moreover miRNA expression profiling has further applications in novel anti-fibrosis therapy in CH.

## Materials and Methods

### Sample preparation

105 liver tissues samples from chronic hepatitis C patients (genotype 1b) were obtained by fine needle biopsy (Table S1). METAVIR fibrosis stages were F0 in 7 patients, F1 in 57, F2 in 24 and F3 in 17. Patients with autoimmune hepatitis or alcoholic liver injury were excluded. None of the patients were positive for hepatitis B virus associated antigen/ antibody or anti human immunodeficiency virus antibody. No patient received interferon therapy or immunomodulatory therapy prior to the enrollment in this study. We also obtained normal liver tissue from the Liver Transplantation Unit of Kyoto University. All of the patients or their guardians provided written informed consent, and Kyoto University Graduate School and Faculty of Medicine's Ethics Committee approved all aspects of this study in accordance with the Helsinki Declaration.

### RNA preparation and miRNA microarray

Total RNA from cell lines or tissue samples was prepared using a *mir*Vana miRNA extraction Kit (Ambion, Austin, TX, USA) according to the manufacturer's instruction. miRNA microarrays were manufactured by Agilent Technologies (Santa Clara, CA, USA) and 100 ng of total RNA was labeled and hybridized using the Human microRNA Microarray Kit protocol for use with Agilent microRNA microarrays Version 1.5 and Mouse microRNA Microarray Kit protocol for use with Agilent microRNA microarrays Version 1.0. Hybridization signals were detected with a DNA microarray scanner G2505B (Agilent Technologies) and the scanned images were analyzed using Agilent feature extraction software (v9.5.3.1). Data were analyzed using GeneSpring GX 7.3.1 software (Agilent Technologies) and normalized as follows: (i) Values below 0.01 were set to 0.01. (ii) In order to compare between one-color expression profile, each measurement was divided by the 75th percentile of all measurements from the same species. The data presented in this manuscript have been deposited in NCBI's Gene Expression Omnibus and are accessible through GEO Series accession number GSE16922 (human) and accession number GSE19865 (mouse).

### Real-time qPCR for human miRNA

For detection of the miRNA level by real-time qPCR, TaqMan® microRNA assay (Applied Biosystems) was used to quantify the relative expression level of miR-199a (assay ID. 002304), miR-199a* (assay ID. 000499), miR-200a (assay ID. 000502), miR-200b (assay ID. 002251), and U18 (assay ID. 001204) was used as an internal control. cDNA was synthesized using the Taqman miRNA RT Kit (Applied Biosystems). Total RNA (10 ng/ml) in 5ml of nuclease free water was added to 3 ml of 5× RT primer, 10× 1.5μl of reverse transcriptase buffer, 0.15 μl of 100 mM dNTP, 0.19 μl of RNase inhibitor, 4.16 μl of nuclease free water, and 50U of reverse transcriptase in a total volume of 15 μl. The reaction was performed for 30 min at 16°C, 30 min at 42°C, and 5 min at 85°C. All reactions were run in triplicate. Chromo 4 detector (BIO-RAD) was used to detect miRNA expression.

### Animal and Chronic Mouse Liver Injury Model

Each 5 adult (8-week-old) male C57BL/6J mice were given a biweekly intra-peritoneal dose of a 10% solution of $CCl_4$ in olive oil (0.02 ml/g/ mouse) for the first 4 weeks and then once a week

for the next 4 weeks. At week 4, 6 or 8, the mice were sacrificed. Partial livers were fixed, embedded in paraffin, and processed for histology. Serial liver sections were stained with hematoxylin-eosin, Azan staining, Silver (Ag) staining, and Elastica van Gieson (EVG) staining, respectively. Total RNA from mice liver tissue was prepared as described previously. All animal procedures concerning the analysis of liver injury were performed in following the guidelines of the Kyoto University Animal Research Committee and were approved by the Ethical Committee of the Faculty of Medicine, Kyoto University.

### Cell lines and Cell preparation

The human stellate cell lines LX-2, was provided by Scott L. Friedman. LX-2 cells, which viable in serum free media and have high transfectability, were established from human HSC lines [26]. LX-2 cells were maintained in D-MEM (Invitrogen, Carlsbad, CA, USA) with 10% fetal bovine serum, plated in 60 mm diameter dishes and cultured to 70% confluence. Huh-7 and Hela cells were also maintained in D-MEM with 10% fetal bovine serum. HuS-E/2 immortalized hepatocytes were cultured as described previously [27]. LX-2 cells were then cultured in D-MEM without serum with 0.2% BSA for 48 hours prior to TGFβ1 (Sigma-Aldrich, Suffolk, UK) treatment (2.5 ng/ml for 20 hours). Control cells were cultured in D-MEM without fetal bovine serum.

### miRNA transfection

LX-2 cells were plated in 6-well plates the day before transfection and grown to 70% confluence. Cells were transfected with 50 pmol of Silencer® negative control siRNA (Ambion) or double-stranded mature miRNA (Hokkaido System Science, Sapporo, Japan) using lipofectamine RNAiMAX (Invitrogen). Cells were harvested 2 days after transfection.

### Real-time qPCR

cDNA was synthesized using the Transcriptor High Fidelity cDNA synthesis Kit (Roche, Basel, Switzerland). Total RNA (2 μg) in 10.4 μl of nuclease free water was added to 1 μl of 50mM random hexamer. The denaturing reaction was performed for 10min at 65°C. The denatured RNA mixture was added to 4 μl of 5× reverse transcriptase buffer, 2 μl of 10 mM dNTP, 0.5 μl of 40U/μl RNase inhibitor, and 1.1 μl of reverse transcriptase (FastStart Universal SYBR Green Master (Roche) in a total volume of 20 μl. The reaction ran for 30 min at 50°C (cDNA synthesis), and five min at 85°C (enzyme denaturation). All reactions were run in triplicate. Chromo 4 detector (BIO-RAD, Hercules, CA, USA) was used to detect mRNA expression. The primer sequences are follows; MMP13 s; 5′-gaggctccgagaaatgcagt-3′, as; 5′-atgccatcgtgaagtctggt-3′, TIMP1 s; 5′-cttggcttctgcactgatgg-3′, as; 5′-acgctggtataaggtggtct-3′, α1-procollagen s; 5′-aacatgaccaaaaaccaaaagtg-3′, as; 5′-cattgtttcctgtgtcttctgg-3′, and β-actin s; 5′-ccactggcatcgtgatggac-3′, as; 5′-tcattgccaatggtgatgacct-3′. Assays were performed in triplicate, and the expression levels of target genes were normalized to expression of the β-actin gene, as quantified using real-time qPCR as internal controls.

### Statistical analyses

Statistical analyses were performed using Student's *t*-test; *p* values less than 0.05 were considered statistically significant. Microarray data were also statistically analyzed using Welch's test and Bonferroni correction for multiple hypotheses testing.

## Supporting Information

**Figure S1** Time line of the induction of chronic liver fibrosis. Upward arrow indicated administration of olive oil or $CCl_4$. Downward arrow indicates when mice were sacrificed.
(TIF)

**Figure S2** Comparison of the expression level of miR-199 and 200 familes in several cell lines and human liver tissue. Endogenous expression level of miR-199a, 199a*, 200a, and 200b in normal liver and LX2 cell as determined by microarray analysis (Agilent Technologies). Endogenous expression level of same miRNAs in Hela, Huh-7 and, immortalized hepatocyte: HuS-E/2 by previously analyzed data [9].
(TIF)

**Table S1** Clinical characteristics of patients by the grade of fibrosis.
(DOCX)

**Table S2** Extracted human miRNAs related to liver fibrosis.
(DOCX)

**Table S3** Corresponding human and mouse miRNAs.
(DOCX)

**Table S4** Hypothetical miRNA target genes according to in silico analysis.
(DOCX)

## Author Contributions

Conceived and designed the experiments: YM KS. Performed the experiments: YM HT YH NK. Analyzed the data: MT MK. Contributed reagents/materials/analysis tools: YM HT YH NK. Wrote the paper: YM MT AT FM NK TO.

## References


1. Wasley A, Alter MJ (2000) Epidemiology of hepatitis C: geographic differences and temporal trends. Semin Liver Dis 20: 1–16.
2. Shepard CW, Finelli L, Alter MJ (2005) Global epidemiology of hepatitis C virus infection. Lancet Infect Dis 5: 558–567.
3. Gressner AM, Weiskirchen R (2006) Modern pathogenetic concepts of liver fibrosis suggest stellate cells and TGF-beta as major players and therapeutic targets. J Cell Mol Med 10: 76–99.
4. Nilsen TW (2007) Mechanisms of microRNA-mediated gene regulation in animal cells. Trends Genet 23: 243–249.
5. Zamore PD, Haley B (2005) Ribo-gnome: the big world of small RNAs. Science 309: 1519–1524.
6. Pillai RS (2005) MicroRNA function: multiple mechanisms for a tiny RNA? Rna 11: 1753–1761.
7. Ura S, Honda M, Yamashita T, Ueda T, Takatori H, et al. (2009) Differential microRNA expression between hepatitis B and hepatitis C leading disease progression to hepatocellular carcinoma. Hepatology 49: 1098–1112.
8. Yamamoto Y, Kosaka N, Tanaka M, Koizumi F, Kanai Y, et al. (2009) MicroRNA-500 as a potential diagnostic marker for hepatocellular carcinoma. Biomarkers 14: 529–538.
9. Murakami Y, Yasuda T, Saigo K, Urashima T, Toyoda H, et al. (2006) Comprehensive analysis of microRNA expression patterns in hepatocellular carcinoma and non-tumorous tissues. Oncogene 25: 2537–2545.
10. Jin X, Ye YF, Chen SH, Yu CH, Liu J, et al. (2008) MicroRNA expression pattern in different stages of nonalcoholic fatty liver disease. Dig Liver Dis.
11. Ogawa T, Iizuka M, Sekiya Y, Yoshizato K, Ikeda K, et al. (2009) Suppression of type I collagen production by microRNA-29b in cultured human stellate cells. Biochem Biophys Res Commun.
12. Ji J, Zhang J, Huang G, Qian J, Wang X, et al. (2009) Over-expressed microRNA-27a and 27b influence fat accumulation and cell proliferation during rat hepatic stellate cell activation. FEBS Lett 583: 759–766.
13. Wienholds E, Kloosterman WP, Miska E, Alvarez-Saavedra E, Berezikov E, et al. (2005) MicroRNA expression in zebrafish embryonic development. Science 309: 310–311.

14. Landgraf P, Rusu M, Sheridan R, Sewer A, Iovino N, et al. (2007) A mammalian microRNA expression atlas based on small RNA library sequencing. Cell 129: 1401–1414.
15. Friedman SL (2008) Hepatic fibrosis-Overview. Toxicology.
16. Roderburg C, Urban GW, Bettermann K, Vucur M, Zimmermann H, et al. (2010) Micro-RNA profiling reveals a role for miR-29 in human and murine liver fibrosis. Hepatology.
17. Venugopal SK, Jiang J, Kim TH, Li Y, Wang SS, et al. (2010) Liver fibrosis causes downregulation of miRNA-150 and miRNA-194 in hepatic stellate cells, and their overexpression causes decreased stellate cell activation. Am J Physiol Gastrointest Liver Physiol 298: G101–106.
18. Jiang J, Gusev Y, Aderca I, Mettler TA, Nagorney DM, et al. (2008) Association of MicroRNA expression in hepatocellular carcinomas with hepatitis infection, cirrhosis, and patient survival. Clin Cancer Res 14: 419–427.
19. Jiang X, Tsitsiou E, Herrick SE, Lindsay MA (2010) MicroRNAs and the regulation of fibrosis. Febs J 277: 2015–2021.
20. Marquez RT, Bandyopadhyay S, Wendlandt EB, Keck K, Hoffer BA, et al. (2010) Correlation between microRNA expression levels and clinical parameters associated with chronic hepatitis C viral infection in humans. Lab Invest.
21. Kim S, Lee UJ, Kim MN, Lee EJ, Kim JY, et al. (2008) MicroRNA miR-199a* regulates the MET proto-oncogene and the downstream extracellular signal-regulated kinase 2 (ERK2). J Biol Chem 283: 18158–18166.
22. Murakami Y, Aly HH, Tajima A, Inoue I, Shimotohno K (2009) Regulation of the hepatitis C virus genome replication by miR-199a. J Hepatol 50: 453–460.
23. Gibbons DL, Lin W, Creighton CJ, Rizvi ZH, Gregory PA, et al. (2009) Contextual extracellular cues promote tumor cell EMT and metastasis by regulating miR-200 family expression. Genes Dev 23: 2140–2151.
24. Gregory PA, Bert AG, Paterson EL, Barry SC, Tsykin A, et al. (2008) The miR-200 family and miR-205 regulate epithelial to mesenchymal transition by targeting ZEB1 and SIP1. Nat Cell Biol 10: 593–601.
25. Oberti F, Valsesia E, Pilette C, Rousselet MC, Bedossa P, et al. (1997) Noninvasive diagnosis of hepatic fibrosis or cirrhosis. Gastroenterology 113: 1609–1616.
26. Xu L, Hui AY, Albanis E, Arthur MJ, O'Byrne SM, et al. (2005) Human hepatic stellate cell lines, LX-1 and LX-2: new tools for analysis of hepatic fibrosis. Gut 54: 142–151.
27. Aly HH, Watashi K, Hijikata M, Kaneko H, Takada Y, et al. (2007) Serum-derived hepatitis C virus infectivity in interferon regulatory factor-7-suppressed human primary hepatocytes. J Hepatol 46: 26–36.

Cancer Epidemiology 34 (2010) 189–193

Contents lists available at ScienceDirect

Cancer Epidemiology

The International Journal of Cancer Epidemiology, Detection, and Prevention

journal homepage: www.cancerepidemiology.net

# Associations between glutathione S-transferase π Ile$^{105}$Val and glyoxylate aminotransferase Pro$^{11}$Leu and Ile$^{340}$Met polymorphisms and early-onset oxaliplatin-induced neuropathy

Masashi Kanai [a,*], Akira Yoshioka [b], Shiro Tanaka [c], Satoshi Nagayama [d], Shigemi Matsumoto [a], Takafumi Nishimura [a], Miyuki Niimi [c], Satoshi Teramukai [c], Ryo Takahashi [d], Yukiko Mori [d], Toshiyuki Kitano [a], Hiroshi Ishiguro [a], Kazuhiro Yanagihara [a], Tsutomu Chiba [a,e], Masanori Fukushima [a,c], Fumihiko Matsuda [f]

[a] Outpatient Oncology Unit, Kyoto University Hospital, 54 Shogoin-Kawahara-cho, Sakyo-ku, Kyoto 606-8507, Japan
[b] Department of Oncology, Mitsubishi Kyoto Hospital, 1 Katsura-gosho-cho, Nishikyo-ku, Kyoto 615-8087, Japan
[c] Translational Research Center, Kyoto University Hospital, 54 Shogoin-Kawahara-cho, Sakyo-ku, Kyoto 606-8507, Japan
[d] Department of Surgery, Kyoto University Hospital, 54 Shogoin-Kawahara-cho, Sakyo-ku, Kyoto 606-8507, Japan
[e] Department of Gastroenterology and Hepatology, Kyoto University Hospital, 54 Shogoin-Kawahara-cho, Sakyo-ku, Kyoto 606-8507, Japan
[f] Department of Genomic Epidemiology, Kyoto University, Yoshida-Konoe-cho, Sakyo-ku, Kyoto 606-8501, Japan

ARTICLE INFO

*Article history:*
Accepted 23 February 2010

*Keywords:*
Oxaliplatin
Neurotoxicity
Colorectal cancer
GSTP1 Ile$^{105}$Val
AGXT Pro$^{11}$Leu
AGXT Ile$^{340}$Met

ABSTRACT

*Purpose:* Although the risk of oxaliplatin-induced neuropathy depends on cumulative oxaliplatin dose, susceptibility to this adverse event differs greatly among patients. In this study, we investigated the associations between oxaliplatin-induced neuropathy and the following polymorphisms: glutathione S-transferase π (*GSTP1*) Ile$^{105}$Val, and glyoxylate aminotransferase (*AGXT*) Pro$^{11}$Leu and *AGXT* Ile$^{340}$Met. *Experimental design:* Eighty-two Japanese patients with histologically confirmed colorectal cancer who received at least six cycles of the modified FOLFOX6 (m-FOLFOX6) regimen were enrolled. To minimize differences in cumulative oxaliplatin dose between patients, oxaliplatin-induced neuropathy was evaluated using an oxaliplatin-specific scale during the 2-week period after completion of the sixth cycle of treatment. *Results:* Forty-four patients developed grade 2/3 oxaliplatin-induced neuropathy. There were more patients carrying at least one *GSTP1* $^{105}$Val allele among the group with grade 2/3 neuropathy (18/44, 41%) than among the group with grade 1 neuropathy (9/38, 24%), although the difference was not statistically significant ($P = 0.098$). There were similar numbers of patients carrying at least one *AGXT* $^{105}$Met allele in the grade 2/3 neuropathy (7/44, 16%) and grade 1 neuropathy groups (5/38, 13%; $P = 0.725$). The *AGXT* $^{11}$Leu allele was not found in any of our patients or controls. *Conclusions:* We found no significant association between oxaliplatin-induced neuropathy and the *GSTP1* Ile$^{105}$Val and *AGXT* Ile$^{340}$Met polymorphisms. Given that no *AGXT* $^{11}$Leu allele was found among our study population ($n = 177$), evaluating this polymorphism in Japanese patients in future studies is likely to be uninformative.



## 1. Introduction

Oxaliplatin, a third-generation diaminocyclohexane platinum compound, is a key drug in the chemotherapeutic treatment of patients with advanced colorectal cancer [1–3]. Oxaliplatin is widely used in palliative settings, and in recent times its efficacy in neoadjuvant and adjuvant settings has also been established, thus an increasing number of colorectal cancer patients are receiving this drug [4,5]. Oxaliplatin often causes neuropathy, which limits the ongoing use of this drug in spite of its wide range of efficacy. The risk of developing oxaliplatin-induced neuropathy depends on cumulative oxaliplatin dose [2,6,7]. However, susceptibility to oxaliplatin-induced neuropathy differs greatly among patients. Some patients suffer from persistent neuropathy for more than 2 years after withdrawal of oxaliplatin, whereas others can tolerate a cumulative oxaliplatin dose of more than 800 mg/m$^2$ without experiencing neuropathy [6–9]. Since there is currently no effective treatment for oxaliplatin-induced neuropathy, risk assessments for this adverse event using a pharmacogenetic approach are clinically valuable.

To date, several genes have been identified as being of interest in the context of the efficacy and toxicity of oxaliplatin.

* Corresponding author. Tel.: +81 75 751 4770; fax: +81 75 751 4772.
*E-mail address:* kanai@kuhp.kyoto-u.ac.jp (M. Kanai).

1877-7821/$ – see front matter © 2010 Elsevier Ltd. All rights reserved.
doi:10.1016/j.canep.2010.02.008

Glutathione S-transferase π (*GSTP1*) is a xenobiotic-metabolizing enzyme involved in the detoxification of a variety of chemotherapeutic drugs, including platinum derivatives [10]. Rs1695, a non-synonymous single nucleotide polymorphism (SNP) of *GSTP1*, converts Ile to Val at codon 105 and reportedly alters the enzymatic activity of the molecule [10–13]. Given that altered *GSTP1* enzyme activity is likely to affect the detoxification of platinum drugs, the association between the *GSTP1* Ile$^{105}$Val polymorphism and clinical response to platinum-based chemotherapy has been examined [14–28]. However, few of these studies were designed to evaluate oxaliplatin-induced neuropathy as a primary endpoint. In one such study, that by Lecomte et al., it was found that grade 3 neuropathy was significantly more frequent among patients harboring the homozygous *GSTP1* $^{105}$Ile allele than among patients with other genotypes. These authors hypothesized that the GSTP1 $^{105}$Ile protein weakens the cell's defenses against oxaliplatin neurotoxicity via inhibition of c-Jun $NH_2$-terminal kinase activity [17]. The results of several other studies support this hypothesis [25,27], whereas other groups have reported no significant association between this genotype and oxaliplatin neurotoxicity [24,26] or have obtained contradictory results [21,28]. Other experimental findings that indirectly challenge the view of Lecomte et al. are that the GSTP1 $^{105}$Val protein is a less potent detoxifier of carcinogens than the GSTP 1 $^{105}$Ile protein [13] and that patients with the Val/Val genotype have been found to receive significant survival benefit from oxaliplatin [14]. Thus, the role of the *GSTP1* Ile$^{105}$Val polymorphism in predicting oxaliplatin-induced neuropathy is still controversial.

Oxaliplatin affects neural voltage-gated sodium channels indirectly via one of its metabolites, oxalate [29,30]. Based on the fact that glyoxylate aminotransferase (AGXT) is involved in the oxalate metabolic pathway [31], Gamelin et al. hypothesized that alterations in *AGXT* genotype and therefore enzyme activity due to *AGXT* genotype could theoretically affect the likelihood of oxaliplatin-induced neuropathy. In fact, they found that the *AGXT* Pro$^{11}$Leu and Ile$^{340}$Met minor polymorphisms are significantly associated with a higher risk of oxaliplatin-induced neuropathy [24].

However, all the above-mentioned studies were carried out using Caucasian patient populations, and to date there have been no such studies performed for Asian patients. There exist considerable interethnic differences in genotype frequency, which can greatly affect the results of pharmacogenetic analyses. For example, the *UGT1A1*28* marker is known to vary markedly between ethnic groups [32–34].

In the present study, we investigated the association between the *GSTP1* Ile$^{105}$Val, *AGXT* Pro$^{11}$Leu and *AGXT* Ile$^{340}$Met polymorphisms and the development of oxaliplatin-induced neuropathy in Japanese colorectal cancer patients. To minimize differences in cumulative oxaliplatin dose, we studied oxaliplatin-induced neuropathy that developed in the 2 weeks after completion of the sixth cycle of m-FOLFOX6.

## 2. Patients and methods

### 2.1. Patients

Between October 2005 and December 2008, a total of 174 patients with histologically confirmed colorectal cancer received at least six cycles of the m-FOLFOX6 regimen at two medical centers. Eighty-two patients (the patients' characteristics are summarized in Table 1) were enrolled in this cohort study. The remaining patients were excluded because they died ($n = 60$), were referred to another hospital ($n = 10$), or were lost to follow-up ($n = 22$) before we could obtain informed consent or a blood sample. The local ethics committees of both centers approved the study protocol. All patients enrolled in this study provided written informed consent. Patient registration and data management were conducted at a data center at Kyoto University Hospital (Translational Research Center). Forty-eight of the 82 patients were chemonaïve and the others had previously undergone at least one chemotherapy regimen other than oxaliplatin-based chemotherapy before m-FOLFOX6 (see Table 1 for details). None of the patients had a history of diabetic neuropathy, but two patients had a history of spondylosis. The m-FOLFOX6 regimen consists of 85 mg/m$^2$ oxaliplatin plus a 400 mg/m$^2$ bolus of 5-fluorouracil and 200 mg/m$^2$ L-leucovorin on day 1, and thereafter a 46-h infusion of 2400 mg/m$^2$ 5-fluorouracil every 2 weeks [35]. The dose and schedule for m-FOLFOX6 were adjusted at the discretion of individual physicians according to baseline bone marrow function or the occurrence of adverse events during the previous cycle. Bevacizumab was concomitantly administered to two patients. Blood tests and physical examinations, including evaluation of oxaliplatin-induced neuropathy, were performed before each cycle. Instances of oxaliplatin-induced neuropathy that occurred during the 2 weeks after completion of the sixth cycle of m-FOLFOX6 were graded using an oxaliplatin-specific scale (grade 1: paresthesia, dysesthesia of short duration; grade 2: paresthesia, dysesthesia persisting between cycles; grade 3: paresthesia, dysesthesia causing functional impairment) [6,36]. In this study, we classified patients without paresthesia or dysesthesia into the grade 1 group.

**Table 1**
Patient characteristics ($n = 82$).

| Variable | $n$ (%) |
|---|---|
| **Gender** | |
| Male | 51 (62) |
| Female | 31 (38) |
| **Age (years)** | |
| Median | 64 |
| Range | 41–80 |
| **Location of primary lesion** | |
| Colon | 47 (57) |
| Rectum | 35 (43) |
| **Histology** | |
| Well-differentiated | 11 (13) |
| Moderately differentiated | 58 (71) |
| Poorly differentiated | 1 (1) |
| Other | 12 (15) |
| **History of prior chemotherapy** | |
| None | 48 (59) |
| Yes | 34 (41) |
| **Previous chemotherapy regimen**[a] | |
| UFT/Uzel | 17 |
| 5-FU/leucovorin | 9 |
| TS-1 | 7 |
| FOLFIRI | 5 |
| UFT | 5 |
| Other | 3 |
| **Cumulative oxaliplatin dose (mg/m$^2$)** | |
| Median | 510 |
| Range | 336–510 |

[a] Several patients received more than one regimen.

### 2.2. DNA extraction and genotyping

Genomic DNA was extracted from whole blood using the phenol–chloroform extraction method and stored at 4 °C until use. The *GSTP1* Ile$^{105}$Val, *AGXT* Pro$^{11}$Leu and *AGXT* Ile$^{340}$Met genotypes were determined by using a fluorescence quenching probe (QProbe, Bex Co., Ltd., Tokyo, Japan) [37,38]. Briefly, a QProbe contains cytosine at its 5′ or 3′ end, which is labeled with a fluorophore that is quenched by guanine. When a QProbe

**Table 2**
Genotype and allele frequencies for the investigated polymorphisms.

| Polymorphism | rs ID | Nucleotide | | Amino acid | | Sample set | Genotype distributions (%) | | | Freq. A2 | *P*-Value[a] |
|---|---|---|---|---|---|---|---|---|---|---|---|
| | | ref. (A1) | var. (A2) | ref. | var. | | A1/A1 | A1/A2 | A2/A2 | | |
| *GSTP1* Ile$^{105}$Val | rs 1695 | A | G | Ile | Val | Grade 2/3 | 26 (59.1) | 17 (38.6) | 1 (2.3) | 0.216 | |
| | | | | | | Grade 1 | 29 (76.3) | 8 (21.0) | 1 (2.6) | 0.132 | 0.158 |
| | | | | | | Control[b] | 68 (73.9) | 21 (22.8) | 3 (3.2) | 0.147 | 0.155 |
| *AGXT* Ile$^{340}$Met | rs 4426527 | A | G | Ile | Met | Grade 2/3 | 37 (84.1) | 6 (13.7) | 1 (2.3) | 0.091 | |
| | | | | | | Grade 1 | 33 (86.8) | 5 (13.2) | 0 | 0.066 | 0.553 |
| | | | | | | Control[b] | 82 (91.1) | 8 (8.9) | 0 | 0.044 | 0.132 |

| Polymorphism | Sample set | Genotype distribution | | *P*-Value[a] | Odds ratio[c] (95% CI) | References |
|---|---|---|---|---|---|---|
| | | A1/A1 | A1/A2 + A2/A2 | | | |
| *GSTP1* Ile$^{105}$Val | Grade 2/3 | 26 | 18 | | | [14,16] |
| | Grade 1 | 29 | 9 | 0.098 | 2.23 (0.86–5.82) | |
| | Control[b] | 68 | 24 | 0.080 | 1.96 (0.92–4.20) | |
| *AGXT* Ile$^{340}$Met | Grade 2/3 | 37 | 7 | | | [23] |
| | Grade 1 | 33 | 5 | 0.725 | 1.25 (0.36–4.31) | |
| | Control[b] | 82 | 8 | 0.226 | 1.94 (0.66–5.74) | |

[a] *P*-values are calculated for grade 2/3 vs. grade 1 or grade 2/3 vs. control.
[b] A sample set representing a control population of healthy Japanese subjects was used.
[c] Odds ratios are calculated for grade 2/3 vs. grade 1 or grade 2/3 vs. control.

hybridizes with the target DNA, its fluorescence is quenched by the guanine in the target that is complementary to the modified cytosine. By monitoring fluorescence intensity, each genotype can be determined. The frequencies of the three SNPs in the general Japanese population were also examined using DNA samples from healthy Japanese volunteers in Pharma SNP Consortium (Tokyo, Japan) [39]. This population is referred to hereafter as the control Japanese population. The investigators performing the genetic analysis were blinded to the patients' characteristics and clinical condition. The characteristics and frequencies of the studied polymorphisms are shown in Table 2.

### 2.3. Statistical analysis

The primary endpoint of the study was the association between genotype distribution and the occurrence of grade 2/3 oxaliplatin-induced neuropathy during the 2 weeks after completion of the sixth cycle of m-FOLFOX6 treatment. The planned sample size ($n = 82$) was specified in the protocol to provide 80% power to detect an odds ratio (OR) of 5.4. The calculations were based on a previous finding that the OR of developing grade 3 oxaliplatin-induced neuropathy in a patient without the *GSTP1* $^{105}$Val allele was 5.54 [17]. We estimated that the frequency of patients in our Japanese population with at least one *GSTP1* $^{105}$Val allele was 21% and used estimated incidences of grade 2/3 oxaliplatin-induced neuropathy after the first six cycles of m-FOLFOX6 for patients with and without a *GSTP1* $^{105}$Val allele of 30% and 70%, respectively. Statistical analysis was performed using a two-sided $\chi^2$/Fisher's exact test with a significance level of 5%, and quantified by calculating ORs with 95% confidence intervals (95% CI). All statistical analysis was conducted using SAS (version 9.13, SAS Institute Inc., Cary, NC).

## 3. Results

Patient characteristics are summarized in Table 1. The median cumulative dose of oxaliplatin was 510 mg/m$^2$ (range, 336–510 mg/m$^2$). Although some patients received a lower cumulative dose than expected, the most common cause of dose adjustment was neutropenia and none of our patients underwent a dose reduction because of neurotoxicity. Forty-four patients (54%) developed grade 2/3 oxaliplatin-induced neuropathy (as scored using the oxaliplatin-specific scale) during the 2 weeks after completion of the sixth cycle of m-FOLFOX6. No significant differences in age, gender or cumulative oxaliplatin dose were observed between the group of patients with grade 2/3 neuropathy and those with grade 1 neuropathy (Table 3).

We performed genotyping analysis for the rs1695, rs34116584 and rs4426527 SNPs, which correspond, respectively, to the *GSTP1* Ile$^{105}$Val, *AGXT* Pro$^{11}$Leu and *AGXT* Ile$^{340}$Met polymorphisms. We performed this analysis for 44 patients with grade 2/3 neuropathy (group A) and 38 patients with grade 1 neuropathy (group B). The frequencies of the variant allele in rs1695 (G), corresponding to *GSTP1* $^{105}$Val, were 0.216 for group A and 0.132 for group B. Although the frequency was higher in group A, the difference was not statistically significant ($P = 0.158$) (Table 2). The frequency of allele G in the control Japanese population was 0.147, which is similar to that of group B. When a dominant model for the variant allele (G) was applied for comparison, the number of patients carrying at least one variant allele was higher in group A (18/44, 41%) than in group B (9/38, 24%) although the difference was not statistically significant ($P = 0.098$) (Table 2). A similar trend was observed when the same comparison between group A and the control Japanese population was performed ($P = 0.080$) (Table 2).

**Table 3**
Association between clinical variables and genotypes and oxaliplatin-induced neuropathy.

| | n (%) | | | *P*[a] |
|---|---|---|---|---|
| | Grade 1 | Grade 2 | Grade 3 | |
| **Age (years)** | | | | |
| <60 | 15 (62) | 9 (38) | 0 (0) | 0.13 |
| ≥60 | 23 (40) | 34 (59) | 1 (2) | |
| **Gender** | | | | |
| Male | 27 (53) | 24 (47) | 0 (0) | 0.11 |
| Female | 11 (36) | 19 (61) | 1 (3) | |
| **Cummulative oxaliplatin dose (mg/m$^2$)** | | | | |
| <510 | 18 (49) | 18 (49) | 1 (3) | 0.50 |
| 510 | 20 (44) | 25 (56) | 0 (0) | |
| **GSTP1 Ile$^{105}$Val** | | | | |
| Ile/Ile | 29 (52) | 26 (47) | 0 (0) | 0.16 |
| Ile/Val | 8 (32) | 16 (64) | 1 (4) | |
| Val/Val | 1 (50) | 1 (50) | 0 (0) | |
| **AGXT Ile$^{340}$Met** | | | | |
| Ile/Ile | 33 (48) | 36 (51) | 1 (1) | 1.00 |
| Ile/Met | 5 (45) | 6 (55) | 0 (0) | |
| Met/Met | 0 (0) | 1 (100) | 0 (0) | |

[a] Fisher's exact test.

**Table 4**
Findings from published studies on *GSTP1* Ile$^{105}$Val and oxaliplatin-induced neuropathy among patients with colorectal cancer.

| Study | Year | Sample size | Ethnicity | Regimen | Cumulative oxaliplatin dose (mg/m$^2$) | Genotype distributions (%) | | | Genotype associated with frequent neuropathy | *P*-Value |
|---|---|---|---|---|---|---|---|---|---|---|
| | | | | | | A1/A1 | A1/A2 | A2/A2 | | |
| Lecomte et al. [17] | 2005 | 64 | Caucasian[a] | Mainly FOLFOX4 (72%) | ≥500 | 39 (61) | 20 (31) | 5 (8) | A1/A1 | 0.02 |
| Grothey et al. [28] | 2005 | 288 | Caucasian | FOLFOX4 | ≤600 | 120 (42) | 130 (45) | 38 (13) | A1/A2 + A2/A2 | 0.03 |
| Ruzzo et al. [21] | 2007 | 166 | Caucasian | FOLFOX4 | N/A | 92 (55) | 62 (37) | 12 (8) | A2/A2 | <0.001 |
| Gamelin et al. [24] | 2007 | 122 | Caucasian | FOLFOX4 | 255–2125 | 54 (44) | 56 (46) | 12 (10) | ns | ns |
| Pare et al. [25] | 2008 | 126 | Caucasian | FOLFOX4 | ≥510 | 44 (35) | 49 (49) | 20 (16) | A1/A1 | 0.08 |
| Kweekel et al. [26] | 2009 | 56 | Caucasian | XELOX | ≥500 | 25 (45) | 25 (45) | 6 (11) | ns | ns |
| Current study | 2009 | 82 | Japanese | m-FOLFOX6 | ≤510 | 55 (67) | 25 (30) | 2 (2) | A1/A2 + A2/A2 | 0.1 |

N/A, not applicable; ns, not significant; XELOX regimen consists of 130 mg/m$^2$ oxaliplatin plus 1000 mg/m$^2$ capecitabine b.i.d. every 3 weeks.
[a] Except four African patients and one Asian patient.

The G allele of SNP rs4426527, corresponding to *AGXT* Ile$^{340}$Met, was present at frequencies that were not significantly different in group A and group B ($P = 0.553$) (Table 2). The T allele of SNP rs34116584, corresponding to *AGXT* $^{11}$Leu, was absent in group A, group B and the control Japanese population ($n = 177$, data not shown). The frequencies of *GSTP1* Ile$^{105}$Val and *AGXT* Ile$^{340}$Met were in Hardy–Weinberg equilibrium.

## 4. Discussion

In this study, to minimize differences in cumulative oxaliplatin dose among patients, we attempted to evaluate oxaliplatin-induced neuropathy during the 2 weeks after completion of the sixth cycle of m-FOLFOX6. As a result, we evaluated early-onset neuropathy rather than the most severe grade of neuropathy that is associated with oxaliplatin.

Lecomte et al. reported that grade 3 oxaliplatin-induced neuropathy, as scored using the oxaliplatin-specific scale, was significantly more frequent among patients harboring the homozygous *GSTP1* $^{105}$Ile allele [17]. Our planned sample size of 82 was based on these findings. In contrast to the findings of Lecomte et al., we found that grade 2/3 neuropathy was more common among patients harboring at least one *GSTP1* $^{105}$Val allele, although the difference was not statistically significant (OR, 2.23; 95% CI, 0.86–5.82; $P = 0.098$; Table 2). There are several possible reasons for this discrepancy between the outcomes of two studies. As mentioned above, our findings reflect our focus on early-onset neuropathy, while Lecomte et al. studied the most severe grade of neuropathy experienced during oxaliplatin treatment. Our findings are in line with those of Grothey et al., who determined that patients harboring at least one *GSTP1* $^{105}$Val allele were more likely to experience early-onset oxaliplatin-induced grade 2/3 neuropathy [28]. Because Grothey et al. studied neuropathy that developed before the cumulative oxaliplatin dose reached 600 mg/m$^2$, their approach is more similar to ours than that of Lecomte et al. Since functional impairment due to oxaliplatin neuropathy does not necessarily develop in a progressive manner but develops suddenly in some patients [40], it is possible that those who are prone to developing early-onset neuropathy have different genotypes from those who suffer from functional impairment due to oxaliplatin neuropathy.

Genetic differences related to ethnic background may also be a reason for the differences between the present results for Japanese patients and the previous results for Caucasian patients. In particular, because of the very low frequency of the *GSTP1* 105 Val/Val genotype among our patients as well as the control Japanese population, we cannot accurately assess the role of this genotype in predicting the likelihood of oxaliplatin-induced neuropathy. Previously published data on the *GSTP1* Ile$^{105}$Val polymorphism and oxaliplatin neurotoxicity are summarized in Table 4.

There has been only one prior study in which the associations between *AGXT* genotypes and oxaliplatin-induced neuropathy have been investigated [24]. In contrast to the findings of Gamelin et al., we did not see any significant association between oxaliplatin-induced neuropathy and the *AGXT* Ile$^{340}$Met polymorphism. This might also be explained by differences in genetic background. In particular, no patients harbored the *AGXT* $^{11}$Leu allele in our study, whereas 30% of patients were found to harbor at least one *AGXT* $^{11}$Leu allele in a Caucasian patient population [24]. In contrast to other clinical responses, such as tumor shrinkage or neutropenia, oxaliplatin-induced neuropathy is minimally affected by concomitantly administered drugs or genetic changes in the tumor cell, so genetic polymorphisms are particularly relevant in the context of susceptibility to oxaliplatin-induced neuropathy. In future pharmacogenetic studies, in order to obtain the most consistent results, we recommend that early-onset neuropathy be evaluated separately from the most severe neuropathy and inter-patient differences in cumulative oxaliplatin dose be minimized.

In summary, we found no significant associations between oxaliplatin-induced neuropathy during the 2-week period after the completion of six cycles of m-FOLFOX6 and the *GSTP1* Ile$^{105}$Val and *AGXT* Ile$^{340}$Met polymorphisms in Japanese colorectal cancer patients. Since no patients harbored the *AGXT* $^{11}$Leu allele in the present study, it seems likely that evaluating this polymorphism in Japanese patients in future studies will not be informative.

## Conflict of interest statement

None declared.

## Acknowledgements

This work was supported by a Grant-in-Aid for Young Scientists (70432416) from the Japan Society for the Promotion of Science. We thank Yoko Teraguchi and Hiroe Tada for their valuable support.

## References

[1] de Gramont A, Vignoud J, Tournigand C, Louvet C, Andre T, Varette C, et al. Oxaliplatin with high-dose leucovorin and 5-fluorouracil 48-hour continuous infusion in pretreated metastatic colorectal cancer. Eur J Cancer 1997;33:214–9.
[2] de Gramont A, Figer A, Seymour M, Homerin M, Hmissi A, Cassidy J, et al. Leucovorin and fluorouracil with or without oxaliplatin as first-line treatment in advanced colorectal cancer. J Clin Oncol 2000;18:2938–47.
[3] Tournigand C, Andre T, Achille E, Lledo G, Flesh M, Mery-Mignard D, et al. FOLFIRI followed by FOLFOX6 or the reverse sequence in advanced colorectal cancer: a randomized GERCOR study. J Clin Oncol 2004;22:229–37.
[4] Andre T, Boni C, Mounedji-Boudiaf L, Navarro M, Tabernero J, Hickish T, et al. Oxaliplatin, fluorouracil, and leucovorin as adjuvant treatment for colon cancer. N Engl J Med 2004;350:2343–51.
[5] Nordlinger B, Sorbye H, Glimelius B, Poston GJ, Schlag PM, Rougier P, et al. Perioperative chemotherapy with FOLFOX4 and surgery versus surgery alone for resectable liver metastases from colorectal cancer (EORTC Intergroup trial 40983): a randomised controlled trial. Lancet 2008;371:1007–16.